Macromolecules

ARTICLE

pubs.acs.org/Macromolecules

Poly(vinylidene fluoride) Graft Copolymer Membranes with "Clickable" Surfaces and Their Functionalization

Tao Cai, K. G. Neoh, and E. T. Kang*

Department of Chemical & Biomolecular Engineering, National University of Singapore, Kent Ridge, Singapore 119260

Supporting Information

ABSTRACT: PVDF-*g*-PPMA copolymers bearing pendant propargyl functionalities were prepared by thermally induced graft copolymerization of propargyl methacrylate (PMA) from the ozone-preactivated poly(vinylidene fluoride) (PVDF) backbones. Microporous membranes were fabricated from the PVDF-*g*-PPMA comb copolymers by phase inversion in aqueous media. The PVDF-*g*-PPMA membrane and pore surfaces with pendant propargyl moieties from the PPMA side chains could be further functionalized via the one-step surface-initiated thiol−yne click reaction or alkyne−azide click reaction. The electrolyte-responsive PVDF-*g*-P[PMA-*click*-MPS] membranes were prepared via thiol−yne click reaction with 3-mercapto-1-propanesulfonic acid sodium salt (MPS) on the microporous PVDF-*g*-PPMA membranes. The permeability of aqueous solutions through the PVDF-*g*-P[PMA-*click*-MPS] membranes exhibited a dependence on the electrolyte concentration. The PVDF-*g*-P[PMA-*click*-*β*-CD] membranes were synthesized via the alkyne−azide click reaction of mono(6-azido-6-desoxy)-*β*-cyclodextrin (azido-*β*-CD) on the PVDF-*g*-PPMA membranes. The PVDF-*g*-P[PMA-*click*-*β*-CD-*guest*-PEO] membranes, from surface inclusion complexation of *diadamantyl*-poly(ethylene oxide) (*AD*-PEO) guest polymer with the *β*-cyclodextrin (*β*-CD) host molecules, exhibited good resistance to protein adsorption and fouling under continuous-flow conditions.

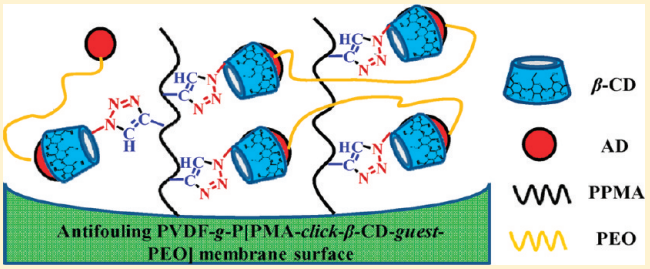

1. INTRODUCTION

Poly(vinylidene fluoride) (PVDF) is a polymer of technological importance because of its unique ferroelectric, piezoelectric, and dielectric properties, good biocompatibility, and excellent membrane forming capability, among others.[1−4] The ability to manipulate and control the surface properties of PVDF is of crucial importance to its widespread applications. The incorporation of desirable functionalities onto PVDF surfaces can be accomplished via several modification methods, such as ozonization,[5] plasma treatment,[6] electron beam (EB) exposure,[7] and surface-initiated controlled radical polymerizations.[8−12]

Covalent attachment of functional molecules or polymer brushes on solid substrates through postpolymerization coupling reactions is another effective method of surface modification, which can be used to prepare functional surfaces that are inaccessible by direct polymerizations of the corresponding monomers. In particular, "click chemistry" including alkyne−azide click reaction,[13−15] and thiol−ene and thiol−yne click reactions,[16,17] have attracted considerable interest because of their high efficiency. The ease of synthesis of the thiol, alkyne, and azide functionalities, coupled with the tolerance for a wide range of functional groups and reaction conditions, makes these coupling processes highly attractive for the modification of polymeric materials and solid substrates.[18]

It would be ideal if the surface of PVDF membranes could be covalently modified with functional groups or well-defined polymer brushes of controlled length and density. The surface-grafted chains could be tailored to impart, for example, stimuli-responsive properties onto the resulting membranes. The click coupling techniques have yet to be fully explored for the surface modification of PVDF membranes through the development of better means for incorporating surface "clickable" functionalities. In the present work, we report the synthesis and characterization of PVDF with propargyl methacrylate (PMA) polymer side chains introduced via graft copolymerization of PMA from ozone-preactivated PVDF in solution. The PVDF-*g*-PPMA copolymer can be readily cast into microporous membranes by phase inversion in an aqueous medium. The graft copolymer membranes with active propargyl groups on the membrane and pore surfaces can be further functionalized via surface-initiated thiol−yne click reaction or alkyne−azide click reaction. In the presence of surface propargyl groups,[19−25] the PVDF-*g*-PPMA copolymer membranes thus provide a unique platform for tailoring the surface functionality and performance of the membranes via one-step "click" reactions.

2. EXPERIMENTAL SECTION

2.1. Materials. Poly(vinylidene fluoride) (PVDF, Kynar K-761) powders having a molecular weight of 441 000 Da were obtained from

Received: February 7, 2011
Revised: March 31, 2011
Published: May 05, 2011

Scheme 1. Schematic Illustration of the Processes of Ozone Pretreatment, Graft Copolymerization of PVDF with PMA, and Preparation of PVDF-*g*-PPMA Membrane with "Clickable" Surface by Phase Inversion

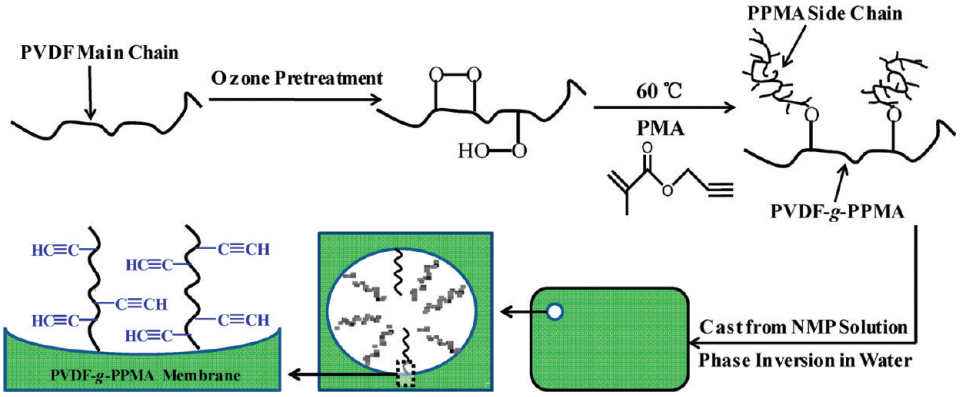

Elf Atochem of North America Inc. Propargyl methacrylate (PMA, Alfa Aesar, 98%) was passed through a inhibitor removing column prior to being stored under an argon atmosphere at −10 °C. Copper(I) bromide (CuBr, Sigma-Aldrich, 99%) was purified by stirring in acetic acid for 4 h, followed by washing thoroughly with ethanol and diethyl ether before being stored under an argon atmosphere. 3-Mercapto-1-propanesulfonic acid sodium salt (MPS, Sigma-Aldrich, 90%), 2,2-dimethoxy-2-phenylacetophenone (DMPA, Sigma-Aldrich, 99%), *N,N,N′,N′,N″*-pentamethyldiethylenetriamine (PMDETA, Sigma-Aldrich, 99%), *N*-methyl-2-pyrrolidone (NMP, Sigma-Aldrich, reagent grade), acetone (Merck, reagent grade), and *N,N*-dimethylformamide (DMF, Merck, HPLC grade) were used as received without further purification. Mono(6-azido-6-desoxy)-β-cyclodextrin (*azido*-β-CD)[26,27] and *diadamantyl*-poly(ethylene oxide)[28] (*AD*-PEO, M_v = 200 000 g/mol) were prepared according to procedures described in the literature. The protein, γ-globulin, was obtained from the Sigma-Aldrich Chemical Co. of St. Louis, MO.

2.2. Thermally Induced Graft Copolymerization of PMA from the Ozone-Pretreated PVDF (PVDF-*g*-PPMA Copolymer). The PVDF powders were first dissolved in NMP to a concentration of 75 g/L. A continuous stream of O_3/O_2 mixture (generated from an Azcozon RMU16-04EM ozone generator) was bubbled through 30 mL of the NMP solution of PVDF at room temperature (~25 °C). The flow rate was adjusted to 300 L/h to give rise to an ozone concentration of about 0.027 g/L in the gaseous mixture. A treatment time of 15 min was used to achieve the desired content of peroxides in the PVDF chains.[29] After ozone preactivation, the polymer solution was cooled in an ice bath, and the activated PVDF was precipitated in excess ethanol. The solution was filtered, and the ozone-treated PVDF was dried by pumping under reduced pressure at ambient temperature.

The functional copolymer was prepared by graft copolymerization of PMA with the ozone-pretreated PVDF (with a peroxide content of about 10^{-4} mol/g)[29] in DMF solution. About 1 g of the ozone-pretreated PVDF was dissolved in 10 mL of DMF. The PMA monomer and DMF solvent were then added to achieve a specific [PMA]/[$-CH_2CF_2-$] molar feed ratio and to adjust the total solution to 20 mL. After an additional 15 min of argon purging, the temperature of the water bath was raised to 60 °C to induce the decomposition of peroxide groups on the PVDF chains and to initiate the graft copolymerization of PMA. After the desired reaction time (6 h), the reactor flask was cooled in an ice bath, and the resultant PVDF-*g*-PPMA copolymer was precipitated in an excess amount of absolute ethanol. The copolymers were purified by redissolving in DMF and reprecipitation in ethanol. The graft copolymers were further purified by extracting with acetone (a good solvent for PPMA homopolymer and a nonsolvent for PVDF) for 48 h in order to remove the residual PPMA, if any. The copolymers were dried under reduced pressure before being subjected to characterization and further reaction. The processes of ozone preactivation of PVDF and thermally induced graft copolymerization of PMA are illustrated in Scheme 1.

2.3. Preparation of Microporous Membranes with Active Surfaces: A Universal Membrane Platform with "Clickable" Alkyne Surfaces. The PVDF and PVDF-*g*-PPMA membranes were prepared by phase inversion of NMP solutions of the respective copolymers in deionized water. The polymer was dissolved in NMP to a concentration of 15 wt % at 50 °C. The solution was cooled to room temperature while stirring continuously. The copolymer solution was then cast onto a glass plate, followed by spreading with a blade to cover the glass plate. The glass plate was subsequently immersed into an aqueous (nonsolvent) coagulation bath of a prescribed temperature for 30 min. The outflow of the solvent and inflow of the nonsolvent resulted in the formation of microporous morphology and the detachment of porous membrane from the supporting glass plate (the phase inversion process). The detached membrane was extracted for another 30 min in the aqueous medium, followed by rinsing twice with deionized water. The purified membranes were obtained by freeze-drying for subsequent characterization and modification. The thickness of the membranes so obtain was about 120 ± 10 μm.

2.4. UV-Initiated Thiol−Yne Click Reaction of MPS on the PVDF-*g*-PPMA Membrane and Pore Surfaces (PVDF-*g*-P[PMA-*click*-MPS] Membranes). The thiol−yne coupling reaction to alkyne-functionalized compounds has been carried out photochemically using DMPA as the initiator.[17] The UV-initiated surface thiol−yne click reaction of 3-mercapto-1-propanesulfonic acid sodium salt (MPS) onto the PVDF-*g*-PPMA membrane and pore surfaces was carried out in a Riko model RH 400-10W rotary photochemical reactor (manufactured by Riko Denki Kogyo of Chiba, Japan). The reactor was equipped with a 1000 W high-pressure Hg lamp and a constant temperature water bath (28 °C). Three pieces of the 2 cm × 2 cm PVDF-*g*-PPMA membranes, MPS (178 mg, 1 mmol), DMPA (5 mg, 0.02 mmol), and doubly distilled water (5 mL) were introduced into a 10 mL single-necked round-bottom flask. A purified argon stream was introduced for 30 min to degas the reaction mixture. The reaction flask was then sealed and subjected to UV irradiation for 1 h. After UV irradiation, the membranes were removed from solution and washed thoroughly with copious amounts of doubly distilled water, followed by freeze-drying overnight. The process of UV-initiated thiol−yne click reaction of MPS and other commercially available thiols (3-mercaptopropioic acid (MPA), mercaptosuccinic acid (MSA), and 2-mercaptoethylamine

dx.doi.org/10.1021/ma2002728 |*Macromolecules* 2011, 44, 4258–4268

Scheme 2. Preparation of Functional PVDF-*g*-P[PMA-*click*-R] Membranes via Surface Thiol−Yne Click Reaction of Thiols on the PVDF-*g*-PPMA Membrane[a]

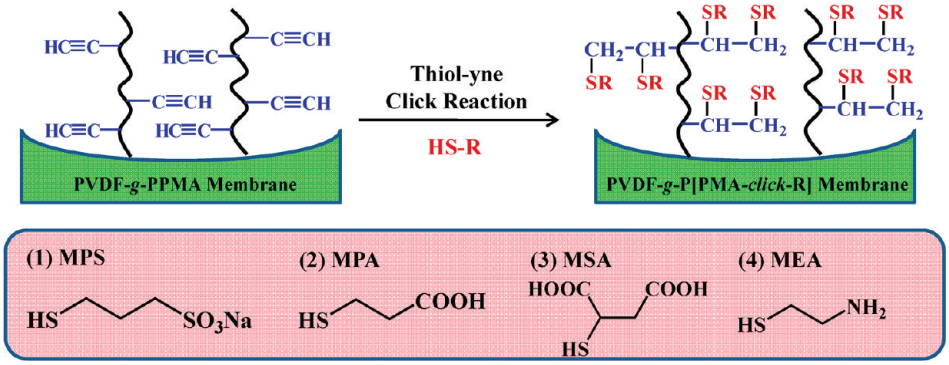

[a] Chemical structures of commercially available thiols (SH-R) employed for the synthesis of functional PVDF membrane: (1) 3-mercapto-1-propanesulfonic acid sodium salt (MPS), (2) 3-mercaptopropionic acid (MPA), (3) mercaptosuccinic acid (MSA), and (4) 2-mercaptoethylamine (MEA).

Scheme 3. Preparation of Functional PVDF-*g*-P[PMA-*click*-R] Membranes via Surface Alkyne−Azide Click Reaction on the PVDF-*g*-PPMA Membrane[a]

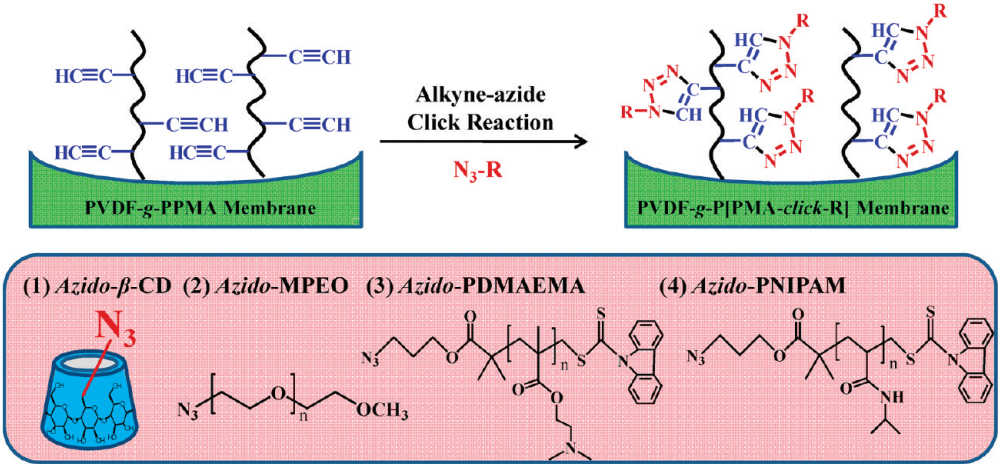

[a] Chemical structures of the synthesized azides (N_3-R) employed for the functionalization of PVDF copolymer membrane: (1) mono(6-azido-6-desoxy)-β-cyclodextrin (*azido*-β-CD), (2) *azido*-poly(ethylene oxide) monomethyl ether (*azido*-MPEO), (3) *azido*-poly[2-(*N*,*N*-dimethylamino)ethyl methacrylate] (*azido*-PDMAEMA), and (4) *azido*-poly(*N*-isopropylacrylamide) (*azido*-PNIPAM).

(MEA), Supporting Information) on the PVDF-*g*-PPMA membrane and pore surfaces is shown in Scheme 2.

2.5. Alkyne−Azide Click Reaction of *Azido*-β-CD on the PVDF-*g*-PPMA Membrane and Pore Surfaces (PVDF-*g*-P[PMA-*click*-β-CD] Membranes). The dormant alkyne end groups on the graft chains provided the sites for modification by "click" reaction.[13−15] Briefly, three pieces of the 2 cm × 2 cm PVDF-*g*-PPMA membranes, *azido*-β-CD (184 mg, 0.16 mmol), and doubly distilled water (10 mL) were introduced into a 25 mL single-necked round-bottom flask. The reaction mixture was degassed with purified argon for about 30 min. PMDETA (8 μL, 0.032 mmol) and CuBr (4.6 mg, 0.032 mmol) were then added to the reaction mixture. The reaction flask was sealed under an argon atmosphere, and the reaction was allowed to proceed at 80 °C for 8 h with stirring. After the reaction, the membranes were removed from solution and washed with copious amounts of hot water (∼80 °C), followed by freeze-drying overnight. The process of surface alkyne−azide click reaction of *azido*-β-CD and other synthesized azides (*azido*-poly(ethylene oxide) monomethyl ether (*azido*-MPEO), *azido*-poly[2-(*N*,*N*-dimethylamino)ethyl methacrylate] (*azido*-PDMAEMA), and *azido*-poly(*N*-isopropylacrylamide) (*azido*-PNIPAM), Supporting Information) onto the PVDF-*g*-PPMA membrane and pore surfaces is shown in Scheme 3.

2.6. Supramolecular Assembly between PVDF-*g*-P[PMA-*click*-β-CD] Membranes and *AD*-PEO Guests. One piece of the 2 cm × 2 cm PVDF-*g*-P[PMA-*click*-β-CD] membrane was immersed into 5 mL of aqueous solution, containing 120 mg of *diadamantyl*-poly(ethylene oxide) (*AD*-PEO) for 12 h under continuous stirring. After removal from the solution, the PVDF-*g*-P[PMA-*click*-β-CD-*guest*-PEO] membrane was immersed in doubly distilled water and washed repeatedly in an ultrasonic bath to precipitate and remove the uncomplexed *AD*-PEO polymer chains, followed by freeze-drying overnight.

2.7. Materials Characterization. Fourier transform infrared (FTIR) spectroscopy analysis of the graft copolymers were carried out on a Bio-Rad FTS 135 Fourier transform infrared spectrophotometer, and the diffuse reflectance spectra were scanned over the range of 400−4000 cm^{-1}. ^1H NMR spectra of the PVDF homopolymer and PVDF-*g*-PPMA copolymer were measured on a Bruker ARX 300 instrument at room temperature with deuterated DMSO as the solvent.

Elemental analyses of the copolymer samples were performed by the Microanalysis Centre of the National University of Singapore. The bulk C contents were determined on a Perkin-Elmer 2400 elemental analyzer. The F contents were determined, on the other hand, by the Schöniger combustion method. The thermal stability of the copolymers was studied by thermogravimetric analysis (TGA). The samples were heated from room temperature to about 700 °C at a heating rate of 10 °C/min under a dry nitrogen atmosphere in a Du Pont Thermal Analyst 2100 system, equipped with a TGA 2050 thermogravimetric thermal analyzer.

X-ray photoelectron spectroscopy measurements were made on a Kratos AXIS Ultra HSA spectrometer with a monochomatized Al Kα X-ray source (1468.6 eV photons). The membranes were mounted on the standard sample studs by means of double-sided adhesive tapes. The core-level signals were obtained at the photoelectron takeoff angle (α, with respect to the sample surface) of 90°. All binding energies (BEs) were referenced to that of the neutral C 1s hydrocarbon peak at 284.6 eV or that of the CF_2 peak of PVDF at 290.5 eV. In peak synthesis, the line width (full width at half-maximum, or fwhm) for the Gaussian peaks was maintained constant for all components in a particular spectrum. Surface elemental stoichiometries were determined from peak-area ratios, after correcting with the experimentally determined sensitivity factors, and were reliable to ±5%. The surface morphology of the microporous membranes was studied by scanning electron microscopy (SEM), using a JEOL 6320 scanning electron microscope. The membranes were mounted on the sample studs by means of double-sided adhesive tapes. A thin layer of palladium was sputtered onto the membrane surface prior to the SEM measurement. The measurements were performed at an accelerating voltage of 15 kV. The average pore diameter and the porosity of the porous membranes were determined by mercury porosimetry (Micromeritics, model Autopore III). Mercury was used as the sole medium, and the pressure applied ranged from 50 to 60 000 psia.

2.8. Measurements of the Electrolyte-Dependent Flux through the Microporous Membranes. The flux of aqueous solutions through the membranes was carried out under an argon pressure of 5.9 kN/m^2. The PVDF-*g*-P[PMA-*click*-MPS] membrane was immersed in the doubly distilled water for several minutes, before being mounted on the microfiltration cell (Toyo Roshi UHP-25, Tokyo, Japan). The effective membrane area was 3.14 cm^2. An aqueous NaCl solution of a specific concentration was added to the cell. The flux was calculated from the weight of the solution permeated per unit time and per unit area of the membrane surface. The microfiltration cell containing the permeate was kept in a thermostated water bath for at least 20 min before the flow was initiated.

2.9. Protein Adsorption Assays. In this work, protein adsorption experiments were carried out on pristine and functionalized PVDF membranes by using γ-globulin as a model protein. The membranes were hydrated in methanol for 30 min initially, followed by washing three times with the phosphate buffer saline (0.01 M PBS, pH 7.4). The pristine or functionalized PVDF membrane was mounted on the microfiltration cell (Toyo Roshi UHP-25, Tokyo, Japan) and exposed to a PBS solution (pH 7.4) containing 2 mg/mL γ-globulin. The flow rate was imposed by an Ar pressure of 9.8 kN/m^2. After the permeation of 1000 mL of the γ-globulin solution, the membrane was removed from the cell and dried under reduced pressure for 24 h. The surface coverage of γ-globulin was quantified by XPS, using the nitrogen signal associated with γ-globulin as a marker. The relative [N]/[C] ratios before and after protein fouling were compared.

3. RESULTS AND DISCUSSION

3.1. Preparation of the Poly(vinylidene fluoride)-*graft*-Poly(propargyl methacrylate) Copolymers (PVDF-*g*-PPMA Copolymers). The process and mechanism of radical-initiated graft copolymerization of vinyl monomers from ozone-pretreated PVDF have been described earlier.[29] Modification of polymer surfaces with alkyne groups is attractive because of the good resistance of the alkyne groups toward the usual addition reaction conditions and attack of functional groups. Yet the alkyne moieties allow the rapid generation of a diverse arrays of functional surfaces via the simple surface alkyne−azide click reaction or thiol−yne click reaction.[18]

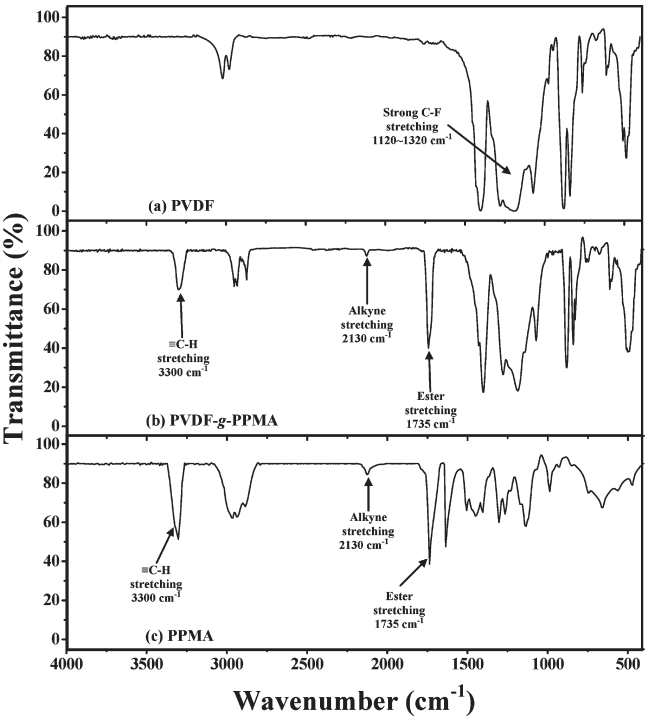

Figure 1. FTIR spectra of the (a) PVDF homopolymer, (b) PVDF-*g*-PPMA copolymer with a $([-PMA-]/[-CH_2CF_2-])_{bulk}$ molar ratio of 0.16, and (c) PPMA homopolymer.

The Fourier transform infrared (FTIR) spectrum of the PVDF-*g*-PPMA copolymer is compared to that of the PPMA homopolymer and that of the PVDF homopolymer in Figure 1a−c. For the PVDF homopolymer, the characteristic absorption band in the wavenumber region of 1120−1280 cm^{-1} is associated with the $-CF_2-$ functional groups of PVDF main chains.[30] On the other hand, three new adsorption bands at the wavenumbers of about 1735, 2130, and 3300 cm^{-1}, associated respectively with the ester stretching, alkyne stretching, and ≡C−H stretching, have appeared after graft copolymerization of propargyl methacrylate (PMA).[30] Thus, the FTIR spectroscopic results are consistent with the presence of grafted PPMA chains on the PVDF backbone.

The bulk graft concentrations of the copolymers can be derived from the carbon-to-fluorine ratio, obtained from elemental analyses. The graft concentration in terms of the number of PMA repeat units per PVDF repeat unit, or the $([-PMA-]/[-CH_2CF_2-])_{bulk}$ molar ratio, can be readily obtained from the $([C]/[F])_{bulk}$ molar ratio by taking into account the carbon stoichiometries of the graft and the main chains and the carbon-to-fluorine ratio of the PVDF main chain. Thus, the $([-PMA-]/[-CH_2CF_2-])_{bulk}$ molar ratio can be calculated from eq 1:

$$([-PMA-]/[-CH_2CF_2-])_{bulk} = (2/7)([C]-[F])_{bulk}/[F]_{bulk} \quad (1)$$

dx.doi.org/10.1021/ma2002728 |*Macromolecules* 2011, 44, 4258–4268

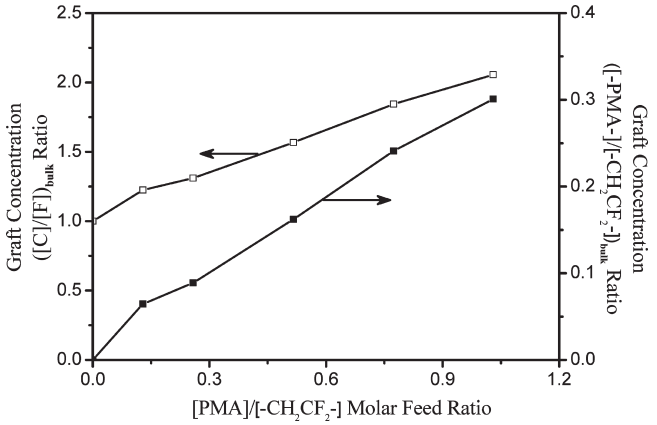

Figure 2. Effect of monomer molar feed ratio (the [PMA]/[$-CH_2CF_2-$] ratio) on the $([C]/[F])_{bulk}$ ratio and bulk graft concentration $([-PMA-]/[-CH_2CF_2-])_{bulk}$ of the PVDF-*g*-PPMA copolymers.

where the factors 2 and 7 are introduced to account for the fact that there are 2 and 7 carbon atoms per repeat unit of PVDF and PPMA, respectively. Figure 2 shows the dependence of the PMA polymer graft concentration in the PVDF-*g*-PPMA copolymer, expressed as the $([C]/[F])_{bulk}$ and $([-PMA-]/[-CH_2CF_2-])_{bulk}$ molar ratios, on the [PMA] to [$-CH_2CF_2-$] molar feed ratio used for the thermally induced graft copolymerization. The graft concentration increases gradually with the increase in PMA monomer concentration used for graft copolymerization.

The chemical structures of the PVDF homopolymer and the PVDF-*g*-PPMA copolymer ($([-PMA-]/[-CH_2CF_2-])_{bulk}$ = 0.16) are verified by ^{1}H NMR spectroscopy in Figure 3. The chemical shifts at δ = 2.2 ppm (***a*1**) and in the range of δ = 2.7−3.0 ppm (***a*2**) in Figure 3a,b are attributable to the head-to-head (hh) or tail-to-tail (tt) stereoregularities and the head-to-tail (ht) bonding arrangements of the PVDF main chains, respectively.[31] Graft polymerization of PMA from PVDF has resulted in the appearance of chemicals shifts in the range of δ = 0.6−0.9 ppm (***c*** in Figure 3b), attributable to the C−CH_3 group of PPMA. The chemical shift at δ = 4.6−4.7 ppm (***d***) is attributable to the $-CO_2CH_2$ species, while the chemical shift at δ = 3.5−3.6 ppm (***e***) is associated with the $-C{\equiv}CH$ species of the PPMA side chains.[31,32] A ratio of about 1:6 for the propargyl protons (***e*** in Figure 3b) to the protons of PVDF main chains (***a*** in Figure 3b) indicates that the bulk molar ratio of PMA segments in the copolymer is about 0.17, which is very close to that obtained from elemental analysis.

Figure 4 shows the respective thermogravimetric analysis (TGA) curves of the PVDF homopolymer (curve a), the three PVDF-*g*-PPMA copolymers of different bulk graft concentrations (curves b, c, and d for $([-PMA-]/[-CH_2CF_2-])_{bulk}$ = 0.09, 0.16, and 0.24, respectively), and the PPMA homopolymer (curve e). In comparison to the PVDF and PPMA homopolymers, a distinct two-step degradation process is observed for the PVDF-*g*-PPMA copolymer samples. The first major weight loss occurring at about 250 °C is attributable to the thermal decomposition of the PPMA segments, while the second major weight loss commencing at about 475 °C is attributable to the thermal decomposition of the PVDF main chains. The extent of the first major weight loss at about 250 °C coincides approximately with the weight content of the PPMA polymer in the respective graft copolymers obtained from elemental analysis. Thus, the TGA

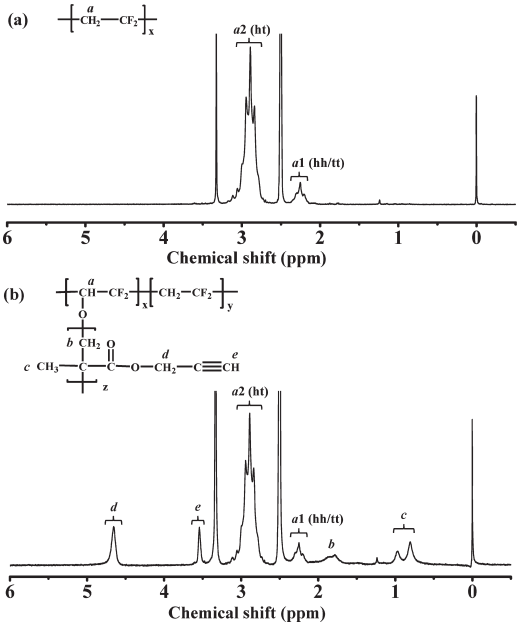

Figure 3. ^{1}H NMR spectra of the (a) PVDF homopolymer and (b) PVDF-*g*-PPMA copolymer with a $([-PMA-]/[-CH_2CF_2-])_{bulk}$ molar ratio of 0.16 in DMSO.

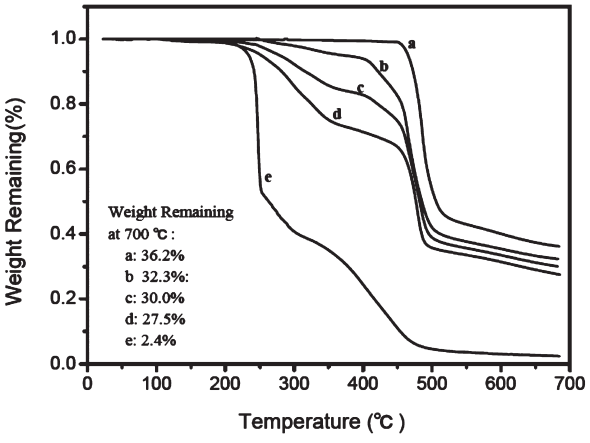

Figure 4. Thermogravimetric analysis curves of (a) the PVDF homopolymer, the PVDF-*g*-PPMA copolymers with $([-PMA-]/[-CH_2CF_2-])_{bulk}$ molar ratios of (b) 0.09, (c) 0.16, (d) 0.24, and (e) the PPMA homopolymer.

results are also consistent with the elemental analysis results and confirm quantitatively the extent of graft copolymerization of PMA from the ozone-pretreated PVDF main chains.

3.2. Preparation of PVDF-*g*-PPMA Copolymer Membranes by Phase Inversion. The PVDF-*g*-PPMA microporous membranes were fabricated by phase inversion of a 15 wt % NMP solution of the PVDF-*g*-PPMA copolymer ($([-PMA-]/[-CH_2CF_2-])_{bulk}$ = 0.16) in doubly distilled water at room temperature. The SEM micrographs in Figure 5a,b illustrate the difference in surface morphology of the microporous membranes cast from the PVDF homopolymer and PVDF-*g*-PPMA copolymer. The SEM images reveal that the PVDF-*g*-PPMA membrane has a more well-defined pore size distribution and a higher degree of porosity, induced by the PPMA graft chains during phase

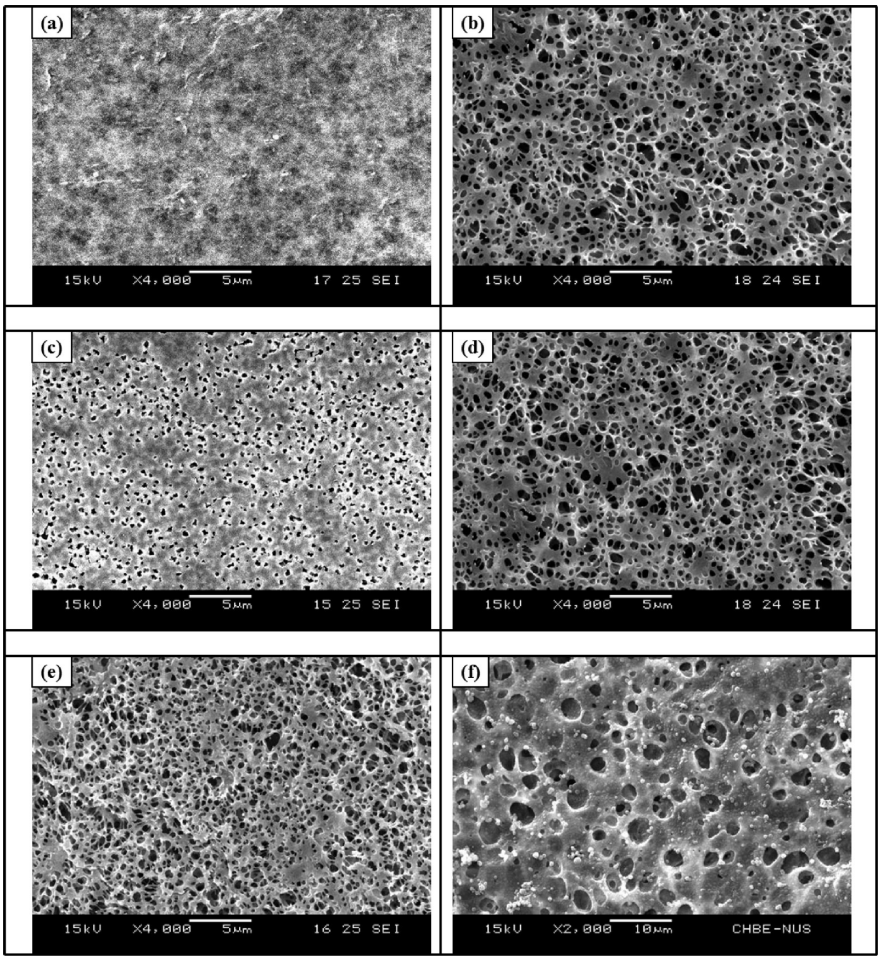

Figure 5. SEM micrographs of the microporous membranes cast from a 15 wt % NMP solution of the corresponding copolymers by phase inversion: (a) the pristine PVDF membrane, (b) the PVDF-*g*-PPMA membrane with a $([-PMA-]/[-CH_2CF_2-])_{surface}$ molar ratio of 0.25, the PVDF-*g*-P[PMA-*click*-MPS] membranes with $([-SO_3^-]/[-CH_2CF_2-])_{surface}$ molar ratios of (c) 0.26, (d) 0.42, (e) 0.53, and (f) PVDF-*g*-P[PMA-*click*-*β*-CD-*guest*-PEO] membrane prepared from PVDF-*g*-PPMA membrane with a $([-PMA-]/[-CH_2CF_2-])_{surface}$ molar ratio of 0.25. All images shown are the surface in contact with the glass substrate during membrane casting by phase inversion.

Table 1. Characterization of the PVDF and PVDF-*g*-PPMA Membranes

membrane sample	$([-PMA-]/[-CH_2CF_2-])_{bulk}$[a]	$([-PMA-]/[-CH_2CF_2-])_{surface}$[b]	average pore diameter (μm)[c]	porosity (%)[c]
PVDF (d = 0.22 μm)[d]			0.56	74
PVDF-*g*-PPMA	0.09	0.15	0.36	51
	0.16	0.25	0.44	75
	0.24	0.32	0.53	88

[a] Derived from the atomic ratio of C and F (obtained from elemental analyses) according to eq 1. [b] Derived from the curve-fitted C 1s peak component area ratio of $[-O-C{=}O]/[C-F_2]$ of the respective sample in Figure 7 since there is one $[C-F_2]$ unit in the PVDF backbone and one $[-O-C{=}O]$ unit in the PPMA side chains. [c] Determined by Hg porosimetry. [d] PVDF microporous membranes obtained from Millipore Corporation. *d* stands for the standard pore size of the commercial hydrophilic and microporous membranes.

inversion, than those of the pristine PVDF membrane. The pore size and porosity of the three PVDF-*g*-PPMA copolymer membranes, determined by mercury porosimetry, are summarized in Table 1. With the increase in PMA graft concentration, the average pore diameter of the PVDF-*g*-PPMA membranes increases from 0.36 to 0.53 μm, and the porosity increases correspondingly from 51% to 88%. The increase in pore size and porosity with the increase in PMA graft concentration confirms that the membrane morphology is dependent on the PMA chain length and is thus controllable. For comparison purposes, a commercial hydrophilic PVDF microporous membrane of comparable pore size and porosity is also included in Table 1.

Figure 6a,b shows the respective wide-scan and C 1s core-level spectra of the pristine PVDF and the PVDF-*g*-PPMA ($([-PMA-]/[-CH_2CF_2-])_{bulk}$ = 0.16) membranes cast by phase inversion. In the case of pristine PVDF membrane (Figure 6a), only C and F signals are observed in the wide-scan

dx.doi.org/10.1021/ma2002728 |*Macromolecules* 2011, 44, 4258–4268

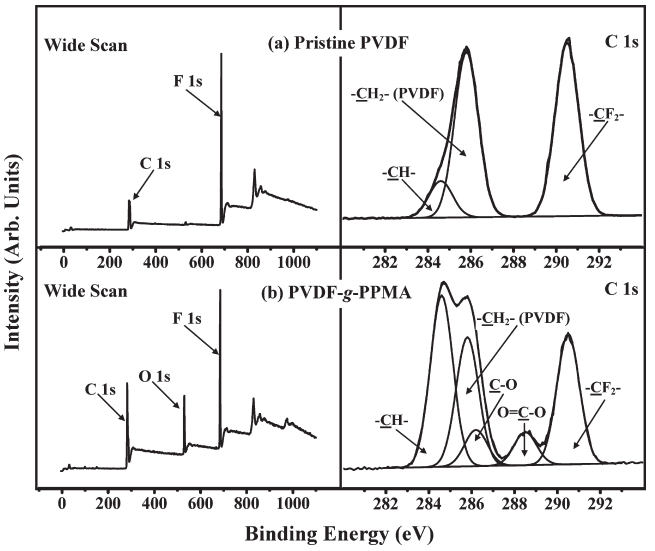

Figure 6. XPS wide-scan and C 1s core-level spectra of the (a) pristine PVDF membrane and (b) PVDF-*g*-PPMA membrane with a $([-PMA-]/[-CH_2CF_2-])_{bulk}$ molar ratio of 0.16.

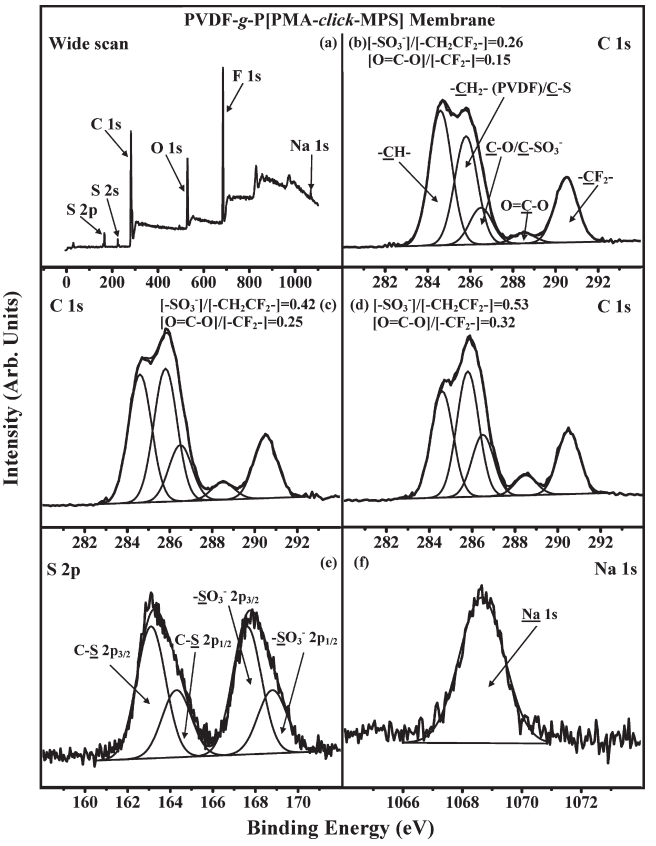

Figure 7. XPS wide-scan, C 1s, S 2p, and Na 1s core-level spectra of three PVDF-*g*-P[PMA-*click*-MPS] microporous membranes with $([-SO_3^-]/[-CH_2CF_2-])_{surface}$ molar ratios of (a, c, e, f) 0.42, (b) 0.26, and (d) 0.53.

spectrum and the C 1s core-level spectrum can be curve-fitted with three peak components, with binding energies (BEs) at 284.6 eV for the neutral *C*H species, 285.8 eV for the CH_2 species (adjacent to the CF_2 species in PVDF), and 290.5 eV for the CF_2 species.[33] The $[-CH_2-]$:$[-CF_2-]$ peak component area ratio of about 1:1 is consistent with the chemical structure of PVDF. For the PVDF-*g*-PPMA membrane, the appearance of a distinctive O 1s signal in the wide-scan spectrum of Figure 6b indicates that PMA has been graft copolymerized from the PVDF main chains. The two new C 1s peak components with BE at 286.2 eV for the *C*−O species and at 288.5 eV for the O−*C*═O species in Figure 6b can also be assigned to the grafted PMA chains. The [*C*−O]:[O−*C*═O] peak component area ratio of about 1:1 is in good agreement with the theoretical ratio based on the chemical structure of PMA. On the other hand, the graft concentration at the membrane surface, or the $([-PMA-]/[-CH_2CF_2-])_{surface}$ ratio of 0.25, as determined from the ([O−*C*═O]/[−CF_2−]) peak component area ratio in the C 1s core-level spectrum of the copolymer membrane in Figure 6b, is higher than the corresponding bulk ratio of 0.16. Thus, surface enrichment of the more hydrophilic PPMA component has occurred in the copolymer membranes during the phase inversion process in the aqueous medium.

3.3. Functionalization of the PVDF-*g*-PPMA Membrane via Click Grafting of 3-Mercapto-1-propanesulfonic Acid Sodium Salt (MPS): Electrolyte-Responsive PVDF-*g*-P[PMA-*click*-MPS] Membrane. Polyelectrolyte brushes can lead to useful surface functionalities, such as superhydrophilicity, antifouling effects, and lubrication properties.[34−37] The thermally induced thiol−yne coupling reaction in the presence of 2, 2-dimethoxy-2-phenylacetophenone (DMPA) was employed for the click grafting of 3-mercapto-1-propanesulfonic acid sodium salt (MPS) on the PVDF-*g*-PPMA membrane to give rise to the PVDF-*g*-P[PMA-*click*-MPS] membrane.[17,21] The presence of click grafted MPS molecules on the PVDF-*g*-P[PMA-*click*-MPS] membrane surface are ascertained by the XPS results. Figure 7a−f shows the respective XPS wide-scan, C 1s, S 2p, and Na 1s core-level spectra of three PVDF-*g*-P[PMA-*click*-MPS] membranes prepared from PVDF-*g*-PPMA membranes with $([PMA]/[-CH_2CF_2-])_{surface}$ molar ratios of 0.15, 0.25, and 0.32. In the wide-scan spectra of the PVDF-*g*-P[PMA-*click*-MPS] membranes, not only are the C 1s, F 1s, and O 1s signals detected, the Na 1s and S 2p signals are also discernible (Figure 7a). With the increase in PMA graft concentration in the starting PVDF-*g*-PPMA copolymer membranes, the $([-SO_3^-]/[-CH_2CF_2-])_{surface}$ molar ratios of the resultant PVDF-*g*-P[PMA-*click*-MPS] membranes increase correspondingly to 0.26, 0.42, and 0.53 (Figure 7b−d). The C 1s core-level spectra are curve-fitted with five peak components. The components with binding energies (BEs) at 284.6, 286.5, and 288.5 eV are attributed to the hydrocarbon backbone, *C*−O/*C*−SO_3^- and O═*C*−O species of the PMA polymer graft chains with clicked MPS.[10,33] The other two peak components at the BEs of 285.8 and 290.5 eV are attributable to the CH_2 and CF_2 species, respectively, of the PVDF main chain. The BE of the *C*−S species (∼285.8 eV) of the MPS moieties overlaps with that of the CH_2 component in the PVDF backbone.[33] In the S 2p core-level spectrum, two spin−orbit split doublets with an area ratios of 1:1 can be identified. The S 2p doublet, with the S $2p_{3/2}$ and $2p_{1/2}$ peak components at the BEs of 163.1 and 164.3 eV, respectively, is associated with the formation of a normal C−*S* bond.[33] On the other hand, the S 2p doublet at the BEs of 167.0 and 168.2 eV can be assigned to the sulfonate C−*S*O_3^- species.[10,33] The surface concentrations of sulfonic acid groups, or the $([-SO_3^-]/[-CH_2CF_2])_{surface}$ ratio, on the PVDF-*g*-P[PMA-*click*-MPS]

dx.doi.org/10.1021/ma2002728 |*Macromolecules* 2011, 44, 4258–4268

membrane can be obtained from the XPS-derived sulfur to fluorine ratio and estimated from eq 2

$$([-SO_3^-]/[-CH_2CF_2-])_{surface} = [S]_{surface}/[F]_{surface} \quad (2)$$

which accounts for the fact that there are two fluorine atoms per repeat unit of the PVDF polymer and two sulfur atoms per unit of the 3-mercapto-1-propanesulfonic acid sodium salt molecules, respectively. The unique feature of the thiol−yne reaction, in comparison to the thiol−ene click reaction, is the ability for an alkyne bond to react with 2 equiv of thiols to form a 1,2-dithioether product (Scheme 2).[17,21] From Table 1 and Figure 7b−d, it can also be seen that the surface concentration of sulfonic acid groups, $([-SO_3^-]/[-CH_2CF_2-])_{surface}$ ratio, is lower than 2 times the corresponding $([-PMA-]/[-CH_2CF_2-])_{surface}$ graft concentration of the starting copolymer membranes. Thus, about 80% of the alkyne groups have undergone the thiol−yne click reaction.

The respective SEM images of PVDF-*g*-P[PMA-*click*-MPS] microporous membranes with $([-SO_3^-]/[-CH_2CF_2-])_{surface}$ molar ratios of 0.26, 0.42, and 0.53, obtained from the corresponding PVDF-*g*-PPMA membranes with $([-PMA-]/[-CH_2CF_2-])_{surface}$ ratio of 0.15, 0.25, and 0.32 (Table 1), are shown in Figure 5c−e. The increase in PPMA graft concentration in the PVDF-*g*-PPMA copolymer also gives rise to the corresponding increase in average pore size and porosity of the PVDF-*g*-PPMA membranes as well as the increase in surface MPS concentration of the PVDF-*g*-P[PMA-*click*-MPS] membranes (Figure 5c−e). Click grafting of MPS onto the PVDF-*g*-PPMA membrane does not appear to cause a significant change in morphology and porosity of the membrane (compare parts b and d of Figure 5).

The electrolyte-dependent flux of aqueous solutions through the PVDF-*g*-P[PMA-*click*-MPS] microporous membranes is shown in Figure 8. Sodium chloride was added to achieve the specific ionic strength of the solution. The flux of the aqueous solution through the PVDF-*g*-P[PMA-*click*-MPS] microporous membranes increases with the increase in electrolyte concentration from 10^{-7} to 10^{-1} mol/L (curves 1−3). On the other hand, the flux of the aqueous solution through the pristine PVDF membrane cast from the 15 wt % NMP solution by phase inversion exhibits an electrolyte-independent behavior (curve 5). The flux of aqueous solution through the commercial hydrophilic PVDF microporous membrane of comparable effective pore size (obtained from Millipore Corp., Bedford, MA) shows only a weak and reversed dependence on the electrolyte concentration of the medium, especially in the high electrolyte concentration range (curve 4).[5]

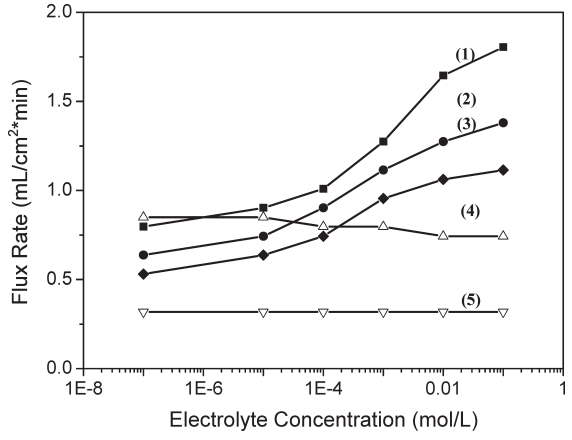

Figure 8. Electrolyte-dependent flux of aqueous solution through the pristine PVDF and PVDF-*g*-P[PMA-*click*-MPS] microporous membranes. Curves 1, 2, and 3 are obtained from three PVDF-*g*-P[PMA-*click*-MPS] microporous membranes with surface graft concentrations ($([-SO_3^-]/[-CH_2CF_2-])_{surface}$ ratios) of 0.53, 0.42, and 0.26, respectively. Curve 4 is the flux through the commercial Millipore hydrophilic PVDF microporous membrane with a standard pore diameter of d = 0.22 μm. Curve 5 is the flux through the membrane cast from the PVDF homopolymer.

The dependence of permeation rate through the PVDF-*g*-P[PMA-*click*-MPS] microporous membrane on the electrolyte concentration is attributable to the conformational change of the P[PMA-*click*-MPS] polymer side chains on the membrane and pore surfaces. At low electrolyte concentrations, the strong electrostatic repulsion among the sulfate anions forces the P[PMA-*click*-MPS] side chains to adopt a highly extended conformation. On the other hand, due to the electrostatic screening effect, a high electrolyte concentration will shield the intrachain and interchain electrostatic repulsion among sulfate anions. The P[PMA-*click*-MPS] graft chains on the membrane and pore surfaces undergo association and aggregation as a result of the polyelectrolyte effect.[38,39] Steric obstruction to transport through the pores of membrane is substantially reduced, resulting in the increased flux through the microporous membrane. This "valve effect" helps to account for flux behavior in the present membrane having relatively short graft chains with no surface aggregation and transmembrane pores with sizes in the micrometer region. The data in Figure 8 also show that the extent of change in permeability of the PVDF-*g*-P[PMA-*click*-MPS] membrane increases with the increase in concentration of the sulfate anions (compare curves 1 and 2 to curve 3), consistent with the "valve effect" exerted by the increasing number of hydrophilic sulfate anions at the solid−fluid interface.[38,39] Since there are no ionic functional groups on the surface of the pristine PVDF membrane, the conformation of the PVDF chains remains unchanged when exposed to aqueous media of different electrolyte concentrations. The weakly electrolyte-dependent flux through the commercial hydrophilic PVDF microporous membrane may have resulted from the functional groups tethered on the membrane surface arising from surface modification.

The radical-mediated coupling reaction of a thiol with an alkyne generates a dithioether adduct as shown in Scheme 2. To explore the efficacy of thiol−yne click reaction on the membrane surfaces, a series of commercially available thiols (Scheme 2 and Supporting Information), including 3-mercaptopropioic acid (MPA), mercaptosuccinic acid (MSA), and 2-mercaptoethylamine (MEA), were selected for the thiol−yne click reactions. All of the resulting membranes exhibit interesting pH-responsive fluxes (Supporting Information, Figure S2).

3.4. Functionalization of the PVDF-*g*-PPMA Membranes via Click Grafting of *Azido*-β-CD: The PVDF-*g*-P[PMA-*click*-β-CD] Membranes. Cyclodextrins (CDs) are toroidally shaped macromolecules with a hydrophilic external surface and a hydrophobic internal cavity, which can form inclusion complexes with shape-compatible organic molecules in aqueous solutions. The complexation behavior between CD hosts and a variety of hydrophobic molecular and polymer guests for mimicking biological recognition, controlled drug release, chiral separation, and polymer synthesis has been widely studied.[40−46] Similar to graft polymerization, immobilization of polymers on a surface via host−guest interaction allows precise control of the nature,

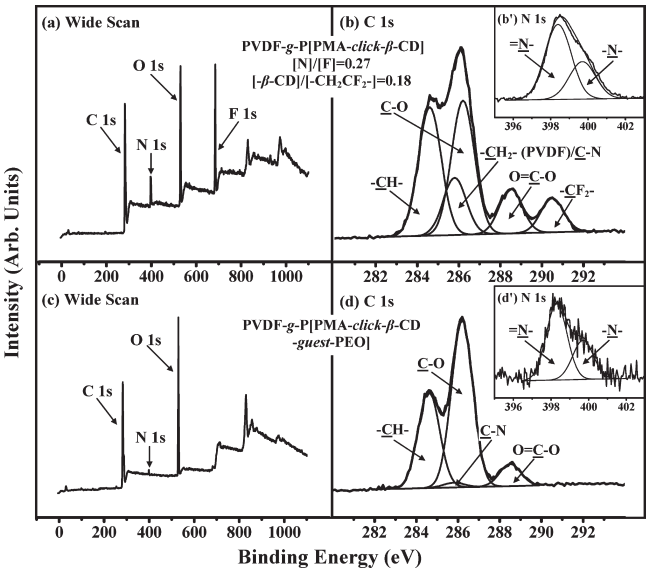

Figure 9. XPS wide-scan, C 1s and N 1s core-level spectra of the (a, b, b′) PVDF-*g*-P[PMA-*click*-β-CD] membrane and (c, d, d′) PVDF-*g*-P[PMA-*click*-β-CD-*guest*-PEO] membrane, from the initial PVDF-*g*-PPMA membrane with a $([-PMA-]/[-CH_2CF_2-])_{surface}$ ratio of 0.25.

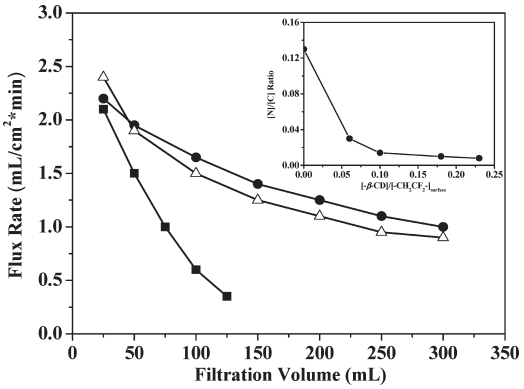

Figure 10. Permeation rate through the Millipore hydrophilic PVDF membrane with a standard pore size of d = 0.22 μm (open triangle, △), PVDF-*g*-PPMA membrane with a $([-PMA-]/[-CH_2CF_2-])_{surface}$ ratio of 0.25 (solid square, ■), and PVDF-*g*-P[PMA-*click*-β-CD-*guest*-PEO] membrane with a $([-\beta\text{-CD}]/[-CH_2CF_2-])_{surface}$ ratio of 0.18 (solid circle, ●) as a function of the filtrate volume of a 2 mg/mL γ-globulin solution under an imposed pressure of 9.8 kN/m^2. Inset: dependence of the extent of γ-globulin adsorption (expressed as the increased [N]/[C] ratio) on the click grafting concentration of β-CD molecules on the PVDF-*g*-P[PMA-*click*-β-CD-*guest*-PEO] membrane after exposure to 1000 mL of γ-globulin solution.

density, and chain length of macromolecules assembled on the surface while still maintaining their original activity.

The surface-initiated alkyne−azide click reaction of mono-(6-azido-6-desoxy)-β-cyclodextrin (*azido*-β-CD) on the PVDF-*g*-PPMA membrane led to the formation of β-CD molecules covalently attached onto the membrane and pore surfaces. Figure 9a shows the XPS wide-scan, C 1s and N 1s core-level spectra of the PVDF-*g*-P[PMA-*click*-β-CD] membrane. In the wide-scan spectrum of the PVDF-*g*-P[PMA-*click*-β-CD] membrane, not only are the C 1s, F 1s, and O 1s signals detected, the N 1s signal is also discernible. The C 1s core-level spectrum of the surface can be curve-fitted into five peak components with BEs at about 284.6, 285.8, 286.2, 288.5, and 290.5 eV, attributable to the *C*−H, $(-CH_2-)_{PVDF}$/*C*−N, *C*−O, O═*C*−O, and $(-CF_2-)_{PVDF}$ species, respectively (Figure 9b).[33] The N 1s core-level spectrum of the PVDF-*g*-P[PMA-*click*-β-CD] membrane can be curve-fitted into two peak components with BEs at 398.4 and 399.7 eV and with an area ratio of 2:1, attributable to the imine nitrogen (=N−) and amine nitrogen (−N−) atoms in the triazole ring, respectively (Figure 9b′).[33] The surface concentrations of β-CD molecules on the PVDF-*g*-P[PMA-*click*-β-CD] membrane, or the $([-\beta\text{-CD}]/[-CH_2CF_2-])_{surface}$ ratio, can be obtained directly from the XPS-derived nitrogen to fluorine ratio, since there are two fluorine atoms per repeat unit of the PVDF polymer and three nitrogen atoms per unit of the triazole ring. The $([-\beta\text{-CD}]/[-CH_2CF_2-])_{surface}$ molar ratio on the PVDF-*g*-P[PMA-*click*-β-CD] membrane is about 0.18, which is lower than the corresponding $([-PMA-]]/[-CH_2CF_2-])_{surface}$ ratio of the starting copolymer membrane (about 0.25), suggesting that about 70% of the alkyne groups have undergone the alkyne−azide click reaction.

The *adamantyl*-modified poly(ethylene oxide) (*AD*-PEO) guests were assembled onto the PVDF-*g*-P[PMA-*click*-β-CD] membrane surface by fitting the adamantane groups inside the cavities of the grafted β-CD molecule.[47] Figure 9c,d,d′ shows the XPS wide-scan, C 1s and N 1s core-level spectra of the PVDF-*g*-P[PMA-*click*-β-CD-guest-PEO] membrane after 12 h of surface inclusion complexation of *AD*-PEO (M_v = 200 000 g/mol). In comparison to the starting PVDF-*g*-P[PMA-*click*-β-CD] membrane (see Figure 9a), marked changes in the XPS wide-scan and C 1s core-level spectra of the PVDF-*g*-P[PMA-*click*-β-CD-*guest*-PEO] membrane are observed. The F signal has disappeared in the wide-scan spectrum, indicating that the PVDF-*g*-P[PMA-*click*-β-CD-*guest*-PEO] membrane surface has been covered by the PEO polymer layer, after surface inclusion of *AD*-PEO polymers, to a thickness beyond the probing depth of the XPS technique (∼7.5 nm for organic matrix[48]). The same result can also be deduced from the changes in the C 1s core-level line shape of the PVDF-*g*-P[PMA-*click*-β-CD-*guest*-PEO] membrane. The two carbon species associated with the PVDF main chains, viz., $(-CH_2-)_{PVDF}$ and $(-CF_2-)_{PVDF}$ with respective BE's at 285.8 and 290.5 eV, have disappeared completely. The spectrum is dominated by the peak component at BE of about 286.2 eV, attributed to the *C*−O species of the assembled *AD*-PEO guest polymer chains. The intensity of the N 1s signal for the PVDF-*g*-P[PMA-*click*-β-CD-*guest*-PEO] membrane has been reduced considerably, in comparison to that of the N 1s signal for the PVDF-*g*-P[PMA-*click*-β-CD] membrane. The XPS results, thus, provide direct evidence on the inclusion of PEO polymer chains on the PVDF-*g*-P[PMA-*click*-β-CD-*guest*-PEO] membrane surface.

The effect of γ-globulin fouling on the permeability of the commercial hydrophilic PVDF membranes, the PVDF-*g*-PPMA membrane, and the PVDF-*g*-P[PMA-*click*-β-CD-*guest*-PEO] membrane was investigated under a fixed filtration pressure of 9.8 kN/m^2 (Figure 10). The permeation rate decreases with the filtrate volume as a result of protein adsorption on the membrane and pore surfaces, compaction of the membrane structure under pressure, and formation of microscopic bubbles in the membranes.[49,50] Initially, the permeation rate of the PVDF-*g*-P[PMA-*click*-β-CD-*guest*-PEO] microporous membrane, with a $([-\beta\text{-CD}]/[-CH_2CF_2-])_{surface}$ ratio of 0.18, is lower than that

of the commercial "low-protein binding" Millipore hydrophilic PVDF membrane of comparable mean pore size. However, when subjected to prolonged flux, the decrease in permeation rate of the PVDF-*g*-P[PMA-*click*-β-CD-*guest*-PEO] membranes become slower because of the good antifouling properties provided by the hydrophilic PEO inclusion layer. On the other hand, the flux of the protein solution through the more hydrophobic PVDF-*g*-PPMA membrane became too low to be measured accurately after the permeation of 150 mL of a 2 mg/mL γ-globulin solution.

The surface composition of the membranes after the permeation of 1000 mL of 2 mg/mL γ-globulin solution was quantified by XPS analysis. The relative amount of surface-adsorbed protein can be expressed simply as the increase in surface [N]/[C] ratio over that arising from the initial alkyne−azide reaction. The dependence of the surface [N]/[C] ratio on the concentration of click-grafted CD molecules of the PVDF-*g*-P[PMA-*click*-β-CD-*guest*-PEO] membranes is summarized in the inset of Figure 10. The level of γ-globulin adsorption on the PVDF-*g*-P[PMA-*click*-β-CD-*guest*-PEO] membrane with a surface [$-\beta$-CD]/[$-CH_2CF_2-$] ratio of 0.06 is less than 25% of that of the corresponding PVDF-*g*-PPMA membrane. The higher the content of β-CD molecules on the membrane surface, the more *AD*-PEO polymer chains are captured, resulting in better antifouling property of the membrane obtained. For membranes with a surface [$-\beta$-CD]/[$-CH_2CF_2-$] ratio of 0.1 and above, the amount of γ-globulin adsorption is significantly decreased. These results indicate that the antifouling property of the membrane has been greatly enhanced after the surface inclusion complexation of the *AD*-PEO guest.

Because of the good efficiency of the alkyne−azide click reaction, polymers bearing pendant azide moieties can be tailored for a wide-range of applications, as shown in Scheme 3. To demonstrate the versatility of these membrane surfaces, a series of azides of interest have been synthesized and studied (Scheme 3 and Supporting Information). Thus, click grafting of *azido*-poly(ethylene oxide) monomethyl ether (*azido*-MPEO), *azido*-poly[2-(*N*,*N*-dimethylamino)ethyl methacrylate] (*azido*-PDMAEMA), and *azido*-poly(*N*-isopropylacrylamide) (*azido*-PNIPAM) on the PVDF-*g*-PPMA membranes have produced, respectively, antifouling, pH-responsive, and temperature-responsive membranes (Supporting Information, Figures S2 and S3).

4. CONCLUSIONS

PVDF-*g*-PPMA copolymers with pendant alkyne moieties in the PPMA side chains were synthesized via graft copolymerization of PMA from the ozone-preactivated PVDF backbones. The microporous membranes prepared from the PVDF-*g*-PPMA copolymers of different graft concentrations by phase inversion in an aqueous medium showed enrichment of the propargyl groups on the membrane and pore surfaces. The PVDF membranes with surface-enriched propargyl groups serve as a "clickable" platform for tailoring the surface functionalities via thiol−yne click reaction of thiol-functionalized molecules, such as MPS, or alkyne−azide click reaction of azide-functionalized macromolecules, such as *azido*-β-CD. The obtained PVDF-*g*-P[PMA-*click*-MPS] membranes exhibited electrolyte-dependent permeability for aqueous solutions, while the PVDF-*g*-P[PMA-*click*-β-CD] exhibited resistance to protein adsorption after surface inclusion of the *AD*-PEO guest polymers. The "surface-clickable" membranes allow the incorporation of a library of thiol-functionalized compounds or azido-functionalized polymers to the membrane and pore surfaces, thus providing a universal platform for functionalization of PVDF membranes.

■ ASSOCIATED CONTENT

Supporting Information. Experimental details on the synthesis of functional PVDF membranes via click reactions, XPS wide-scan spectra of the respective copolymer membranes, and pH-dependent flux and temperature-dependent flux through the respective copolymer membranes. This material is available free of charge via the Internet at http://pubs.acs.org.

■ AUTHOR INFORMATION

Corresponding Author

*Tel +65-65162189; Fax +65-67791936; e-mail cheket@nus.edu.sg.

■ REFERENCES

(1) Li, K. *Chem. Eng. Technol.* **2002**, *25*, 203–206.
(2) Souzy, R.; Ameduri, B.; Boutevin, B. *Prog. Polym. Sci.* **2004**, *29*, 75–106.
(3) Junginckel, B. J. In *The Polymeric Materials Encyclopedia*; Salamone, J. C., Ed.; CRC Press: Boca Raton, FL, 1996; Vol. 7, pp 7114−7123.
(4) Seiler, D. A. In *Modern Fluoropolymers; PVDF in the Chemical Process Industry*; Scheirs, J., Ed.; Wiley: New York, 1997; Chapter 25, pp 487−506.
(5) Zhai, G. Q.; Toh, S. C.; Tan, W. L.; Kang, E. T.; Neoh, K. G. *Langmuir* **2003**, *19*, 7030–7037.
(6) Chang, Y.; Chang, W. J.; Shih, Y. J.; Wei, T. C.; Hsiue, G. H. *ACS Appl. Mater. Interfaces* **2011**10.1021/am200055k.
(7) Holmberg, S.; Lehtinen, T.; Nasman, J.; Ostrovoskii, D.; Paronen, M.; Serimaa, R.; Sundholm, F.; Sundholm, G.; Torell, G.; Torkkeli, M. *J. Mater. Chem.* **1996**, *6*, 1309–1317.
(8) Hester, J. F.; Banerjee, P.; Won, Y. Y.; Akthakul, A.; Acar, M. H.; Mayes, A. M. *Macromolecules* **2002**, *35*, 7652–7661.
(9) Akthakul, A.; Hochbaum, A. I.; Stellacci, F.; Mayes, A. M. *Adv. Mater.* **2005**, *17*, 532–535.
(10) Zhai, G. Q.; Kang, E. T.; Neoh, K. G. *Macromolecules* **2004**, *37*, 7240–7249.
(11) Chen, Y. W.; Ying, L.; Yu, W. H.; Kang, E. T.; Neoh, K. G. *Macromolecules* **2003**, *36*, 9451–9457.
(12) Ameduri, B. *Chem. Rev.* **2009**, *109*, 6632–6686.
(13) (a) Kolb, H. C.; Finn, M. G.; Sharpless, K. B. *Angew. Chem., Int. Ed.* **2001**, *40*, 2004–2021. (b) Lewis, W. G.; Green, L. G.; Grynszpan, F.; Radic, Z.; Carlier, P. R.; Taylor, P.; Finn, M. G.; Sharpless, K. B. *Angew. Chem., Int. Ed.* **2002**, *41*, 1053–1057. (c) Hawker, C. J.; Wooley, K. L. *Science* **2005**, *309*, 1200–1205.
(14) (a) Huisgen, R. *Angew. Chem., Int. Ed.* **1963**, *2*, 633–696. (b) Huisgen, R. *Angew. Chem., Int. Ed.* **1968**, *7*, 321–328. (c) Huisgen, R. *1, 3-Dipolar Cycloaddition Chemistry*; Wiley: New York, 1984; Vol. 1.
(15) Golas, P. L.; Matyjaszewski, K. *Chem. Soc. Rev.* **2010**, *39*, 1338–1354.
(16) Hoyle, C. E.; Bowman, C. N. *Angew. Chem., Int. Ed.* **2010**, *49*, 1540–1573.
(17) Hoyle, C. E.; Lowe, A. B.; Bowman, C. N. *Chem. Soc. Rev.* **2010**, *39*, 1355–1387.
(18) Iha, R. K.; Wooley, K. L.; Nystrom, A. M.; Daniel, J. B.; Kade, M. J.; Hawker, C. J. *Chem. Rev.* **2009**, *109*, 5620–5686.
(19) Ishizu, K.; Tsubaki, K.; Mori, A.; Uchida, S. *Prog. Polym. Sci.* **2003**, *28*, 27–54.
(20) Hoogenboom, R. *Angew. Chem., Int. Ed.* **2010**, *49*, 3415–3417.
(21) Hensarling, R. M.; Doughty, V. A.; Chan, J. W.; Patton, D. L. *J. Am. Chem. Soc.* **2009**, *131*, 14673–14675.

(22) Chen, G. J.; Kumar, J.; Gregory, A.; Stenzel, M. H. *Chem. Commun.* **2009**, *41*, 6291–6293.
(23) Fairbanks, B. D.; Scott, T. F.; Kloxin, C. J.; Anseth, K. S.; Bowman, C. N. *Macromolecules* **2009**, *42*, 211–217.
(24) Fairbanks, B. D.; Sims, E. A.; Anseth, K. S.; Bowman, C. N. *Macromolecules* **2010**, *43*, 4113–4119.
(25) Chan, J. W.; Hoyle, C. E.; Lowe, A. B. *J. Am. Chem. Soc.* **2009**, *131*, 5751–5753.
(26) Wu, J. Y.; He, H. K.; Gao, C. *Macromolecules* **2010**, *43*, 2252–2260.
(27) Trellenkamp, T.; Ritter, H. *Macromolecules* **2010**, *43*, 5538–5543.
(28) Zhang, Z. X.; Liu, X.; Xu, F. J.; Loh, X. J.; Kang, E. T.; Neoh, K. G.; Li, J. *Macromolecules* **2008**, *41*, 5967–5970.
(29) Wang, P.; Tan, K. L.; Kang, E. T.; Neoh, K. G. *J. Mater. Chem.* **2001**, *11*, 783–789.
(30) *The Systematic Identification of Organic Compounds*, 7th ed.; Shriner, R. L., Hermann, C. K. E., Morrill, T. C., Curtin, D. Y., Fuson, R. C., Eds.; J. Wiley & Sons: New York, 1998.
(31) Pham, Q.-T.; Petiaud, R.; Llauro, M.-F.; Waton, H. *Proton and Carbon NMR Spectra of Polymers*; John Wiley & Sons: Chichester, UK, 1984; Vol. 3, p 455.
(32) Munteanu, M.; Choi, S. W.; Ritter, H. *Macromolecules* **2008**, *41*, 9619–9623.
(33) *The Handbook of X-ray Photoelectron Spectroscopy*, 2nd ed.; Moulder, J. F., Stickle, W. F., Sobol, P. E., Bomben, K., Eds.; Perkin-Elmer Corporation (Physical Electronics): Wellesley, MA, 1992; pp 216−217.
(34) Terayama, Y.; Kikuchi, M.; Kobayashi, M.; Takahara, A. *Macromolecules* **2011**, *44*, 104–111.
(35) Chem, M.; Briscoe, W. H.; Armes, S. P.; Klein, J. *Science* **2009**, *323*, 1698–1701.
(36) Kitano, H.; Suzuki, H.; Matsuura, K.; Ohno, K. *Langmuir* **2010**, *26*, 6767–6774.
(37) Matsuda, Y.; Kobayashi, M.; Annaka, M.; Ishihara, K.; Takahara, A. *Langmuir* **2008**, *24*, 8772–8778.
(38) Lowe, A. B.; McCormick, C. L. In *Stimuli-Responsive Water Soluble and Amphiphilic Polymers*, 2nd ed.; McCormick, C. L., Ed.; American Chemical Society: Washington, DC, 2000; Vol. 780, pp 1−13.
(39) McCormick, C. L.; Kathmann, E. E. In *The Polymeric Materials Encyclopedia*; Salamone, J. C., Ed.; CRC Press: Boca Raton, FL, 1996; Vol. 7, pp 7189−7201.
(40) Meng, H.; Xue, M.; Xia, T.; Zhao, Y. L.; Tamanoi, F.; Stoddart, J. F.; Zink, J. I.; Nel, A. E. *J. Am. Chem. Soc.* **2010**, *132*, 12690–12697.
(41) Van de Manakker, F.; Vermonden, T.; Van Nostrum, C. F.; Hennink, W. E. *Biomacromolecules* **2009**, *10*, 3157–3175.
(42) Dos Santos, J. F. R.; Alvarez-Lorenzo, C.; Silva, M.; Balsa, L.; Couceiro, J.; Torres-Labandeira, J. J.; Concheiro, A. *Biomaterials* **2009**, *30*, 1348–1355.
(43) Osaki, M.; Takashima, Y.; Yamaguchi, H.; Harada, A. *Macromolecules* **2007**, *40*, 3154–3158.
(44) Cinar, H.; Kretschmann, O.; Ritter, H. *Macromolecules* **2005**, *38*, 5078–5082.
(45) Li, L.; Guo, X. H.; Wang, J.; Liu, P.; Prud'homme, R. K.; May, B. L.; Lincoln, S. F. *Macromolecules* **2008**, *41*, 8677–8681.
(46) Wenz, G.; Gruber, C.; Keller, B.; Schilli, C.; Albuzat, T.; Muller, A. *Macromolecules* **2006**, *39*, 8021–8026.
(47) Zhao, Q.; Wang, S. F.; Cheng, X, J.; Yam, R. C. M.; Kong, D. L.; Li, R. K. Y. *Biomacromolecules* **2010**, *11*, 1364–1369.
(48) Tan, K. L.; Woon, L. L.; Wong, H. K.; Kang, E. T.; Neoh, K. G. *Macromolecules* **1993**, *26*, 2832–2836.
(49) Wavhal, D. S.; Fisher, E. R. *Langmuir* **2003**, *19*, 79–85.
(50) Karabelas, A. J.; Mourouzidis-Mourouzis, S. A. *J. Membr. Sci.* **2008**, *323*, 17–27.